Desalination and Water Treatment
www.deswater.com

doi: 10.5004/dwt.2017.20571

74 (2017) 326–335
May

High surface area mesoporous activated carbon developed from coconut leaf by chemical activation with H_3PO_4 for adsorption of methylene blue

Ali H. Jawad[a,*], Ramlah Abd Rashid[a], Khudzir Ismail[a], S. Sabar[b]

[a]*Coal and Biomass Energy Research Group, Faculty of Applied Sciences, Universiti Teknologi MARA, 40450 Shah Alam, Selangor, Malaysia, Tel. +60355211721; Fax: +60355444562; emails: ahjm72@gmail.com, ali288@salam.uitm.edu.my (A.H. Jawad), Tel. +60124872038; email: d_chemist@yahoo.com (R.A. Rashid), Tel. +60355444562; email: khudzir@salam.uitm.edu.my (K. Ismail)*
[b]*Chemistry Section, School of Distance Education, Universiti Sains Malaysia, 11800 Minden, Penang, Malaysia, Tel. +6046532284; email: sumiyyahs@usm.my*

Received 20 May 2016; Accepted 11 February 2017

ABSTRACT

In this paper, coconut (*Cocos nucifera* L.) leaves, an agricultural waste, were used as precursors to prepare activated carbon by using H_3PO_4-activation method. Physical properties of the prepared activated carbon (PAC) were undertaken using Brunauer–Emmett–Teller (BET), scanning electron microscopy, Fourier transform infrared, elemental analyzer (CHN) and point of zero charge method. Batch mode experiments were conducted to study the influence of the initial pH (3–11), initial dye concentration (30–400 mg/L), contact time (1–300 min) and temperature (303–323 K) on the adsorption of the methylene blue (MB). The kinetic adsorption is well described by the pseudo-second-order model, and the Langmuir model describes the adsorption behavior at equilibrium. The adsorption capacities ($q_{\max}$) of PAC obtained are 357.14, 370.37 and 370.37 mg/g at temperature of 303, 313 and 323 K, respectively. PAC has a mesopore content of 93% with an average pore size of 73.94 Å. The BET surface area and total pore volume corresponded to 981.79 m^2/g and 1.371 cm^3/g, respectively. Various thermodynamic parameters such as standard enthalpy ($\Delta H°$), standard entropy ($\Delta S°$) and standard free energy ($\Delta G°$) showed that the adsorption of MB onto PAC was favorable and endothermic in nature.

Keywords: Activated carbon; Adsorption; Coconut leaves; Biomass; Methylene blue; Phosphoric acid

1. Introduction

Activated carbon (AC) is a carbonaceous material with high porosity and usually used for the removal of chemical species phase (liquid or gas) by adsorption [1,2]. The high adsorptive capacity of activated carbon is related to its surface area, internal porosity, surface structure, pore volume and pore-size distribution [3,4]. These properties have been determined by physical properties and chemical composition of the precursor, activation method, activating agent and the condition of activation process [5,6]. The properties of AC depend on its preparation method along with the nature of the activation method, physical and/or chemical processes [7]. Physical activation involves a two-step process where conversion of the precursor into carbonized material (char) is followed by activation with oxidizing gases such as carbon dioxide, water vapor or their mixtures [8]. In chemical activation, the precursor is impregnated with the activators and simultaneously carbonized at different temperatures. However, both of these conventional methods transfer heat to the carbon particles by conduction or convection which requires high energy consumption and are time consuming in order to obtain the desired activation level [9]. The activating agent helps to develop the activated carbon porosity by dehydration and degradation. Certain dehydrating agent influence temperature of pyrolysis decomposition and inhibit the formation of tar, increasing the carbon yield [10]. Among the numerous activating agents used for chemical activation, H_3PO_4 has been commonly used due to environmental and economic concerns [11].

---

* Corresponding author.

Coconut (*Cocos nucifera*) is a versatile palm tree that belongs to the Arecaceae family with widespread use as a source of food, fuel and raw materials. In Malaysia, coconut is the fourth most important industrial crop after oil palm, rubber and paddy [12]. However, large amounts of coconut waste materials are produced [13]. The utilization of coconut waste by-products such as husks [14], shells [15], fronds [16] and dregs [17] as potential precursors for the production of AC have been studied. Coconut leaves have limited usage and the wastes from natural pruning and silvicultural activities are often left to decompose on the fields that can cause fungi and pest infection. Thus, there is an interest to use these materials as a precursor for AC to yield a value-added adsorbent and to address waste disposal of this abundant resource.

In our previous study, unmodified coconut leaves were successfully used as a potential adsorbent for removal of methylene blue (MB) with a moderate adsorption capacity (112.4 mg/g) [18]. The utility of coconut leaves as a precursor led to the current study to produce activated carbon. In particular, the aim of this work was to prepare a high surface area AC from coconut leaves (prepared activated carbon [PAC]) by using H_3PO_4-activation method. The structural characterization of PAC was performed using gas adsorption, scanning electron microscopy (SEM) and Fourier transform infrared (FTIR) and elemental analyzer (CHN). Whereas, physicochemical parameters were evaluated such as bulk density, ash content, moisture content, iodine number and point of zero charge (pH_{PZC}). The role of porous structure of PAC in adsorption process of selected MB as the model adsorbate at variable adsorbent dosage, pH, initial dye concentration and contact time for this unique biomaterial is considered. Among various cationic dyes, MB is the most frequently used cationic dye for dyeing silk, wood, paper, cotton, wool and temporary hair colorant [19]. The extensive usage of MB can often cause eye burns, which may be a main reason for permanent injury to the eyes of mankind and animals [20]. Moreover, among various wastewater treatment methods, adsorption received great attentions owing to its simplicity of design, high performance and convenient in operating without the production of dangerous end products [21,22].

2. Materials and methods

2.1. Materials

The fallen coconut leaves were collected and used for the preparation of activated carbon at Universiti Teknologi MARA (UiTM), Arau Campus, Perlis, Malaysia. The coconut leaves were cut, washed with tap water to eliminate any contaminants, dried at 100°C for 24 h, before being grinded and sieved to 150–212 μm particle sizes. Phosphoric acid (H_3PO_4) obtained from HmbG Chemicals (Malaysia) was used as the chemical reagent for activation of the coconut leaves. MB dye (chemical formula: $C_{16}H_{18}ClN_3S_3H_2O$, molecular weight: 373.9 g/mol, solubility in water: 40 g/L) purchased from R&M Chemicals (Malaysia) was used as the adsorbate.

2.2. Preparation of activated carbon

The coconut leave based activated carbon (PAC) was prepared by predetermined optimum impregnation ratio of H_3PO_4:biomass (1:3 wt%) with occasional stringing, and then kept in an oven for 24 h at 110°C. The sample was then placed in a stainless steel vertical tubular reactor and put in the furnace. The carbonization process was conducted under high purified nitrogen gas (99.99%) with 700°C under the pressure of 1 atm for 1 h. The activated products were then cooled to room temperature and washed with 3 M of HCl solution followed by hot distilled water until the filtrate turn neutral pH (~pH 7). The PAC was then dried in an oven at 110°C for 24 h. After that, the PAC was ground and the powder was sieved to obtain a particle size range of 150–212 μm. Finally, the PAC was stored in tightly closed bottles for subsequent use. The yield of the activated carbon was calculated by the following Eq. (1):

$$\text{Percentage yield (\%)} = \frac{\text{Wt. of activated carbon}}{\text{Wt. of dried coconut leaves}} \times 100 \quad (1)$$

The physicochemical properties of PAC were calculated through the bulk density, ash content, moisture content, iodine test and pH_{PZC}. Bulk density, ash content, iodine number and moisture content were determined according to procedure described by Ahmed and Dhedan [23], pH_{PZC} is from Makeswari and Santhi [24].

2.3. Characterization of activated carbon

Textural characterization of the PAC was carried out by N_2 adsorption at 77 K using Autosorb I (Quantachrome Corporation, USA). The SEM micrographs of the samples were obtained using Quanta (Leica Cambridge S360). FTIR spectrometer (PerkinElmer , Malaysia) was used to verify the presence of surface functional groups before and after MB adsorption. The elemental analysis was carried out using a CHN analyzer (PerkinElmer, Series II, 2400).

2.4. Batch adsorption experiments

A predetermined amount of selected adsorbents (0.12 g of PAC) was added to 250 mL Erlenmeyer flasks containing 200 mL of MB solution. The flasks were capped and agitated in an isothermal water bath shaker (Memmert, water bath, model WNB7-45, Germany) at fixed shaking speed of 120 strokes/min and 30°C until equilibrium was achieved. Batch adsorption experiments were carried out on common variables of interest such as initial pH (3–11), initial dye concentration (30–400 mg/L) and contact time (1–300 min) to determine the optimum conditions for MB adsorption. The pH of MB solution was adjusted by adding either 0.10 M HCl or 0.10 M NaOH to the desired pH value by monitoring with a pH meter (Metrohm, Model 827 pH Lab, Switzerland). After the stirring, the supernatant was collected with a 0.20 μm Nylon syringe filter and the concentrations of MB were monitored at a different time interval using a HACH DR 2800 Direct Reading Spectrophotometer at a wavelength of 661 nm. For the thermodynamic studies, similar procedures were applied at 313 and 323 K, with the other factors keeping constant. The adsorption capacity at time t, q_t (mg/g), the adsorption capacity at equilibrium, q_e (mg/g) and the percentage of color removal (CR %) of MB were calculated using Eqs. (2)–(4), respectively.

$$q_t = \frac{(C_0 - C_t)V}{W} \quad (2)$$

$$q_e = \frac{(C_0 - C_e)V}{W} \tag{3}$$

$$\text{CR\%} = \frac{(C_0 - C_e)}{C_0} \times 100 \tag{4}$$

where C_o is the initial dye concentration (mg/L); C_t is the dye concentration (mg/L) at time t (min); C_e is the dye concentration at equilibrium (mg/L); V is the volume of dye solution used (mL) and W is the dry mass of the adsorbent used (g). Adsorption experiments were conducted in triplicates under identical conditions and the results are reported as average values.

3. Results and discussion

3.1. Physicochemical properties of PAC

The measured physicochemical properties of PAC are summarized in Table 1. This table shows 35.5% yield of PAC. Moreover, PAC has relatively low bulk density, ash content and moisture content. This observation indicates that PAC has high carbon content, low mineral content or inorganic residue with low water content. PAC also indicates relatively high iodine number with 909 mg/g. On the other hand, PAC has a large Brunauer–Emmett–Teller (BET) surface area (981.79 m^2/g), which is in good agreement with results for mesoporous AC materials obtained from other biomass sources [25,26].

Table 1
Physicochemical characteristics of PAC

Typical properties	
Bulk density (g/mL)	0.14
Iodine number (mg/g)	909
Yield (%)	35.5
Proximate analysis (wt%)	
Ash content	2.33
Moisture content	7.46
Fixed carbon (yield)	35.5
Ultimate analysis (wt%)	
C	63.27
H	2.66
N	Not detected
S	Not detected
O (by difference)	34.07
Textural properties of PAC	
Total pore volume (cm^3/g)	1.371
Micropore volume (cm^3/g)	0.095
Mesopore volume (cm^3/g)	1.276
Average pore size (Å)	73.94
BET surface area (m^2/g)	981.79

3.2. Characterization of PAC

Nitrogen adsorption/desorption curve offers qualitative information on the adsorption mechanism and porous structure of the carbonaceous materials [27]. Fig. 1(a) shows the N_2 adsorption/desorption isotherm of PAC at 77 K with the corresponding pore-size distribution. Based on plotted graph, isotherm profile belongs to the type IV. Type IV isotherm is given by many mesoporous industrial adsorbents and this type indicates the multilayer formation at low pressure after monolayer coverage [28]. The average pore diameter of PAC is approximately 73.94 Å, implying that the structure of PAC is dominated by the mesoporous structure. The International Union of Pure and Applied Chemistry defines the pores based on their pore diameter as micropores (<20 Å), mesopores (20–500 Å) and macropores (>500 Å) [29]. The shape of the PAC adsorbent N_2 adsorption–desorption isotherm (Fig. 1(a)) can also be used to determine what type of hysteresis is present during N_2 adsorption/desorption. Fig. 1(a) can be classified as type IV, it was observed that the curve indicates the presence of H3 type hysteresis loop which is associated with

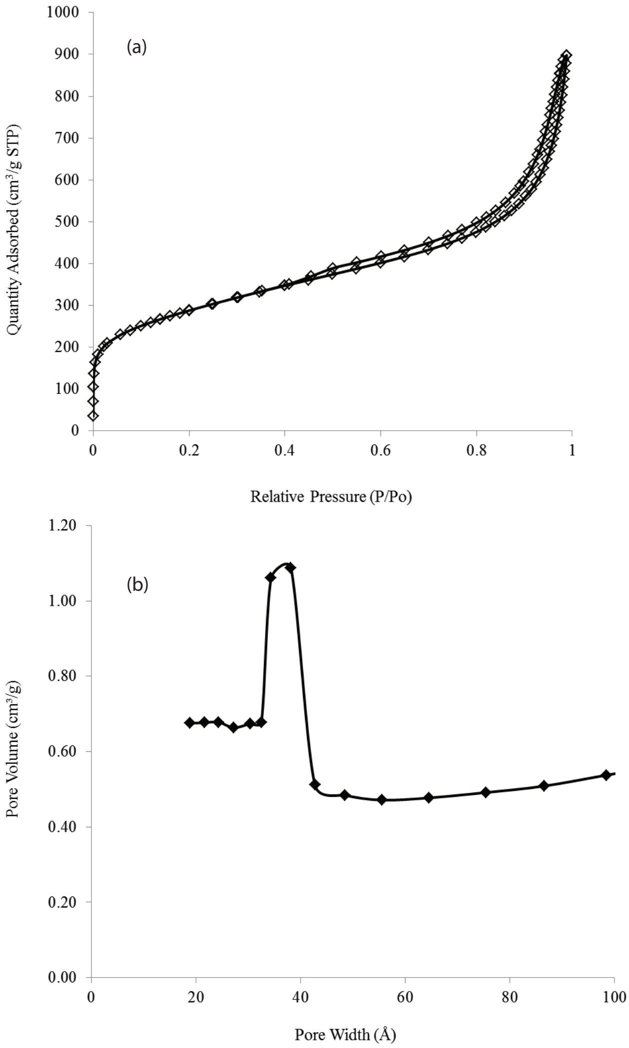

Fig. 1. Textural properties of PAC: (a) isotherms of N_2 adsorption/desorption and (b) pore-size distribution.

capillary condensation that occurs in the mesoporous. The textural parameters are summarized in Table 1 and show that mesopores are prominent since it accounts for 93% of the total pore volume. The pore-size distribution shown in Fig. 1(b) reveals the mesopore character of PAC.

The SEM images of PAC before and after MB adsorption with 3,000× magnifications are presented in Figs. 2(a) and (b), respectively. As observed in micrographs, chemical activation process was useful in developing pore structure within the carbon (Fig. 2(a)). The pores on the surfaces of PAC are resulted from the evaporation of the activating agent during carbonization, leaving behind the ruptured surface of activated carbon with pores previously occupied by the activating agent [30]. The external surface of the activated carbons has cracks and crevices as well as irregular and heterogeneous morphology with a well-developed porous structure in various sizes. Due to the presence of these cavities, large number of MB molecules could easily diffuse and be trapped into the pore structure of PAC. This assumption was supported by Fig. 2(b) where the surface of PAC after MB adsorption became denser and less open pores are seen on the surface of PAC due to adsorption of MB molecules on the PAC surface.

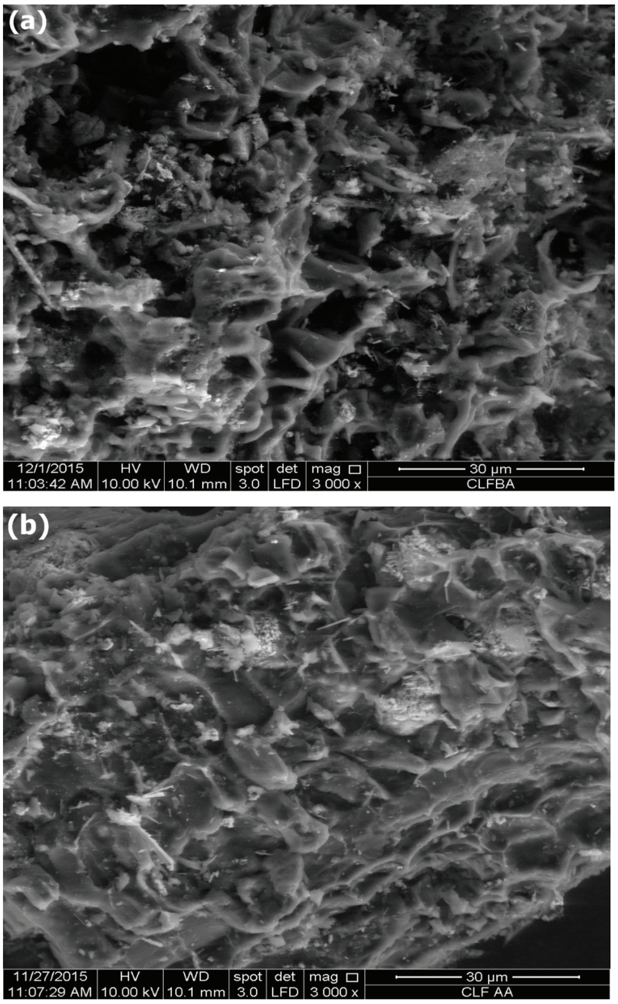

Fig. 2. Typical SEM micrograph of PAC particle (3,000× magnification): (a) before MB adsorption and (b) after MB adsorption.

FTIR analysis of PAC before MB adsorption shows that several adsorption bands are observed in Fig. 3(a). The broad absorption band at 3,300–3,600 cm^{-1} with a maximum at about 3,400 cm^{-1} is characteristic of the stretching vibration of hydrogen-bonded hydroxyl groups (from carboxyls, phenols or alcohols) and water adsorbed in the activated carbons [31]. The band at 1,678 cm^{-1} relates to C=O stretching of ketones, aldehydes, lactones or carboxyl groups, and the band at 1,576 cm^{-1} is assigned to C=C vibrations in aromatic rings [32]. Broad band at 1,000–1,300 cm^{-1} is usually found with oxidized carbons and has been attributed to C–O stretching in acids, alcohols, phenols, ethers and esters. Nevertheless, it is also a characteristic of phosphocarbonaceous and phosphorus compounds present in the phosphoric acid activated carbons [31]. Assignment in this region is difficult because absorption bands from are overlapped. The shoulder at 1,050–1,080 cm^{-1} was assigned to ionized linkage $P^+–O^-$ in acid phosphate esters, and to symmetrical vibration in a P–O–P chain [33]. New bands assigned to anhydride (1,600–1,700 cm^{-1}) and nitro (1,370–1,380 cm^{-1}) are attributed to MB. The bands at 3,400 and 1,080 cm^{-1} shifted to lower bands. Therefore, the functional groups of PAC that likely contribute to interactions with MB cations are the O–H and –COOH Lewis base functional groups.

The charge of PAC surface was identified by pH_{PZC} analysis. The pH_{PZC} of an adsorbent is a very important characteristic that determines the pH at which the adsorbent surface has net electrical neutrality. As shown in Fig. 4, the pH_{PZC} of the PAC obtained was 4.2. Below the pH_{PZC} value, surface of PAC is positively charged, favoring the adsorption of anions, and above the pH_{PZC} value the PAC has a negative surface charge, promoting the adsorption of cations.

3.3. Batch adsorption studies

3.3.1. Effect of pH

The pH solution is expected to influence the adsorption capacity of dyes due to its impact on both the surface binding sites of the adsorbent and the ionization process of the

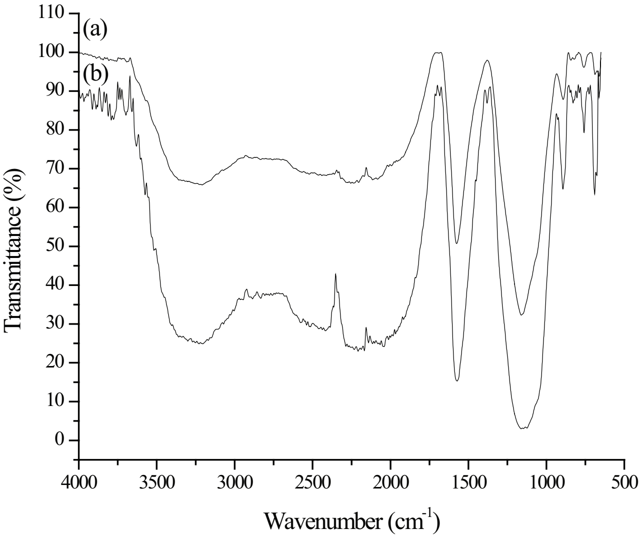

Fig. 3. FTIR spectra of PAC: (a) before MB adsorption and (b) after MB adsorption.

dye molecule. However, as illustrated in Fig. 5, MB uptake (q_e) onto PAC was not affected by pH within the range from 3 to 11 due to buffering effect of the adsorbent [34]. Similar observations have been reported for the adsorption of MB by *Parthenium hysterophorus* [35], *Prosopis cineraria* sawdust [36] and *Posidonia oceanica* (L.) fibers [37]. Therefore, the pH value of unadjusted MB solution (pH 5.6) was used throughout this study.

3.3.2. Effect of initial MB concentration and contact time

The effect of adsorption capacity with contact time was investigated with the initial MB concentration that ranged from 30 to 400 mg/L, as shown in Fig. 6. The amount of MB adsorbed by PAC at equilibrium increased rapidly from 44.70 to 361.49 mg/g with an increase of initial MB concentration from 30 to 400 mg/L. This was attributed to an increase of the collision rate between MB cations and PAC surface at a higher initial dye concentration. Hence, more MB cations were transferred to the PAC surface.

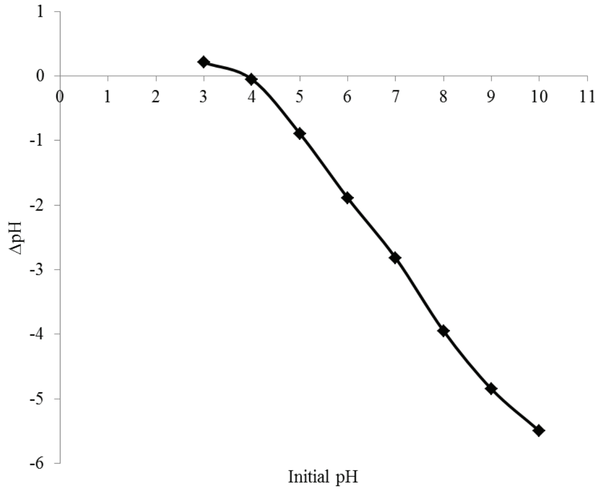

Fig. 4. pHPZC of PAC suspensions.

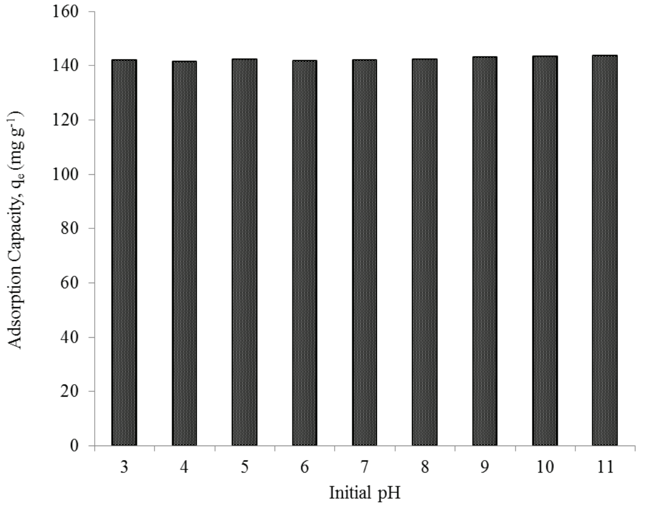

Fig. 5. Effect of pH on the adsorption capacity of MB by PAC ($[MB]_o$ = 100 mg/L, V = 100 mL, T = 303 K, shaking speed = 120 stroke/min, contact time = 60 min and PAC mass = 0.06 g).

3.3.3 Effect of temperature on dye adsorption

Temperature is one of the parameters influenced the adsorption of MB onto PAC. The temperature effect on the adsorption capacity of PAC was studied at 303, 313 and 323 K with the initial concentrations of 30–400 mg/L. Based on the graph plotted in Fig. 7, it is generally observed that the adsorption capacity increase with increasing temperature at all MB concentration studied. This indicates that the adsorption process of MB onto PAC was favored at higher temperature, in agreement with an endothermic adsorption process.

3.4. Adsorption isotherms

The application of adsorption isotherms are useful to predict the interaction between the adsorbate and the adsorbent,

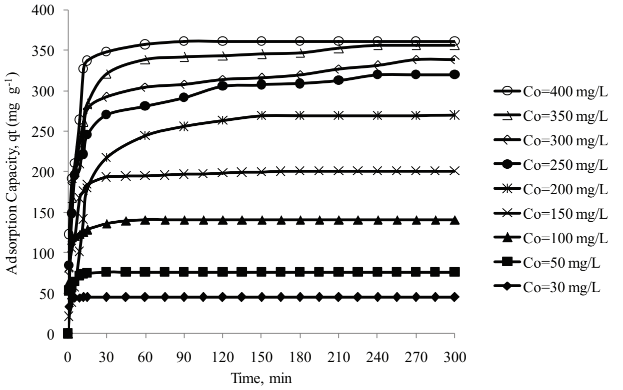

Fig. 6. Effect of initial dye concentration and contact time on the adsorption capacity of MB by PAC (V = 200 mL, pH = 5.6, T = 303 K, shaking speed = 120 stroke/min and PAC mass = 0.12 g).

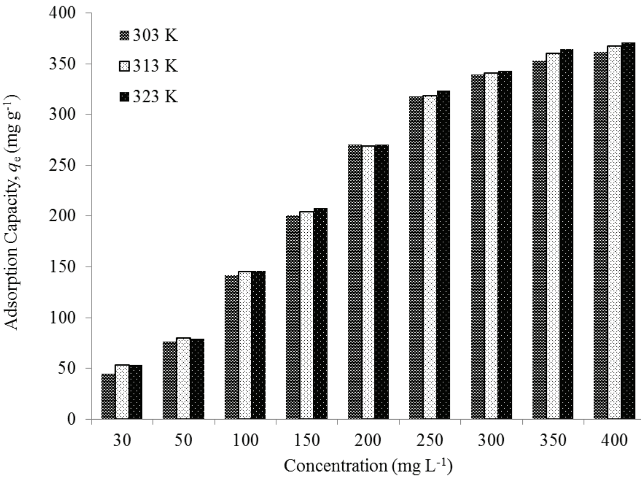

Fig. 7. Effect of temperature on the equilibrium adsorption capacity of PAC at different initial MB concentrations (V = 200 mL, pH = 5.6, shaking speed = 120 stroke/min and PAC mass = 0.12 g).

where the equilibrium distribution of adsorbate molecules occurs between the liquid and solid phases of any system [38]. To quantify the adsorption capacity of PAC for the uptake of the MB dye from aqueous solutions, we tested the Langmuir [39] and Freundlich [40] isotherm models. Langmuir model describes the monolayer adsorption process for uniform adsorption sites and can be expressed in Eq. (5):

$$\frac{C_e}{q_e} = \frac{1}{q_m K_L} + \frac{1}{q_m} C_e \quad (5)$$

where C_e is the equilibrium concentration (mg/L), q_e is the amount adsorbed species per specified amount of adsorbent (mg/g), K_L is the Langmuir equilibrium constant and q_m is the amount of adsorbate required to form an adsorbed monolayer (mg/g). Hence, a plot of C_e/q_e vs. C_e should be a straight line with a slope ($1/q_m$) and an intercept as ($1/q_m\ K_L$) as shown in Fig. 8(a).

Freundlich isotherm describes the multilayer adsorption process on heterogeneous adsorption sites, which can be expressed in Eq. (6):

$$\ln q_e = \ln K_F + \frac{1}{n} \ln C_e \quad (6)$$

where K_F and n are Freundlich constants. K_F (mg/g (L/mg)$^{1/n}$) represents the adsorption capacity and $1/n$ indicates the adsorption intensity and curvature. K_F and n_F can be calculated from the intercept and slope of the plot of lnq_e vs. lnC_e. The plot of lnq_e vs. lnC_e yields a straight line with slope of $1/n$, whereas; K_F was calculated from the intercept value as illustrate in Fig. 8(b). The parameters of these models were calculated and summarized in Table 2 where it is observed that the Langmuir model is found to be linear over the whole concentrations range. Langmuir model assumes that adsorption occurs over a surface with homogeneous energy sites, which are equally available for interaction. However, this statement is only valid for complete monolayer, the transmigration of adsorbate onto adsorbent surface does not occur [41]. Langmuir model provides a better description of the adsorption process according to the R^2 values. The calculated $q_{\max}$ was found to be 357.14, 370.37 and 370.37 mg/g at temperature of 303, 313 and 323 K, respectively. In addition, the $q_{\max}$ of PAC is favorably high in comparison to other activated carbon reported in the literature, as recorded in Table 3. Therefore, PAC has been proven here to be an effective adsorbent and coconut leaves should be a possible precursor for the production of activated carbon.

3.5. Adsorption kinetics

The kinetic adsorption data can be processed to understand the dynamics of the adsorption reactions in terms of the order of the rate constant [41]. The kinetic data were analyzed using two different kinetic models namely pseudo-first-order (PFO) model and pseudo-second-order (PSO) model. The PFO model was proposed initially by Lagergren [47] and its linearized form is expressed by Eq. (7) as follows:

$$\ln(q_e - q_t) = \ln q_e - k_1 t \quad (7)$$

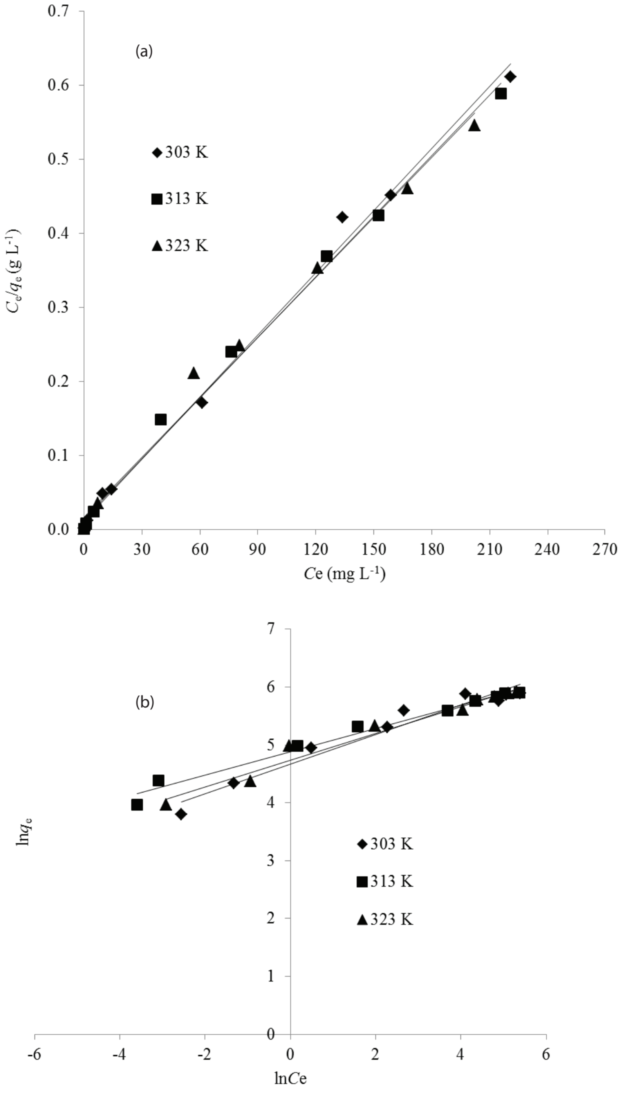

Fig. 8. Isotherm models for the adsorption of MB onto PAC at variable temperature: (a) Langmuir and (b) Freundlich.

Table 2
Isotherm parameters for removal of MB by PAC at variable temperatures

Temperature (K)	Langmuir isotherm		
	q_m (mg/g)	K_L (L/mg)	R^2
303	357.14	0.275	0.995
313	370.37	0.203	0.995
323	370.37	0.165	0.992
Temperature (K)	Freundlich isotherm		
	K_F ((mg/g) (L/mg)$^{1/n}$)	$1/n$	R^2
303	106.62	0.25	0.952
313	131.95	0.20	0.982
323	114.00	0.23	0.970

Table 3
Comparison of adsorption capacities of MB onto different activated carbons prepared by H_3PO_4 activating agent

Adsorbent	Adsorbent dosage (g)	pH	Temperature (K)	BET surface area (m^2/g)	q_{max} (mg/g)	References
Coconut leaves	0.06 g/100 mL	5.6	303–323	981	357.14–370.37	This study
Coffee grounds	0.1 g/100 mL	6	298	1,400	367.0	[33]
Shea cake	0.2 g/100 mL	6	303	1,148	333.33	[42]
Cotton cake	0.2 g/100 mL	6	303	584	250.0	[42]
Cotton stalk	0.4 g/100 mL	6	298	653	245.7	[43]
Jute fiber	0.1 g/100 mL	4	303	–	225.6	[44]
Bamboo	0.1 g/100 mL	6	298	1,335	183.3	[45]
Corn cob	0.02 g/100 mL	8	298	–	28.65	[46]

where q_e (mg/g) and q_t (mg/g) are the amount of MB adsorbed by PAC at equilibrium and time t, respectively; while k_1 (1/min) is the PFO model rate constant.

The values of k_1 and $q_{e,\text{cal}}$ can be estimated from the slope and intercept of $\ln(q_e - q_t)$ vs. t, respectively, as shown in Fig. 9(a). The linear form of the PSO model [48] is described by Eq. (8):

$$\frac{t}{q_t} = \frac{1}{k_2 q_e^2} + \frac{t}{q_e} \tag{8}$$

where k_2 (g/(mg · min)) is the PSO rate constant. The values of k_2 and $q_{e,\text{cal}}$ were calculated from the intercept and slope of t/q_t vs. t, respectively. The plotted graph is shown in Fig. 9(b). The kinetic parameters of the two models are shown in Table 4 along with its linear regression coefficients, R^2, where R^2 values are favorable ($R^2 \geq 0.99$) for the PSO model. Furthermore, the values of $q_{e,\text{cal}}$ are in agreement with the experimental values ($q_{e,\text{exp}}$). Therefore, the PSO model shows a better fit relative to the PFO model for kinetic uptake properties of MB onto PAC. The PSO model was used to evaluate the rate-limiting step controlling the adsorption of MB onto activated carbon derived from palm date seeds [49] and apricot stones [50].

3.6. Adsorption thermodynamics

The adsorption thermodynamics parameters of MB onto PAC were computed from the experimental data conducted at 303, 313 and 323 K. The changes in Gibbs free energy ($\Delta G°$), enthalpy ($\Delta H°$) and entropy ($\Delta S°$) were calculated using the following Eqs. (9)–(11) [51]:

$$K_d = \frac{q_e}{C_e} \tag{9}$$

$$\Delta G° = -RT \ln K_d \tag{10}$$

$$\ln K_d = \frac{\Delta S°}{R} - \frac{\Delta H°}{RT} \tag{11}$$

where K_d is the distribution coefficient, q_e is the concentration of MB adsorbed on PAC at equilibrium (mg/L), C_e is the equilibrium concentration of MB in the liquid phase (mg/L), R is the universal gas constant (8.314 J/(mol K)) and T is the absolute

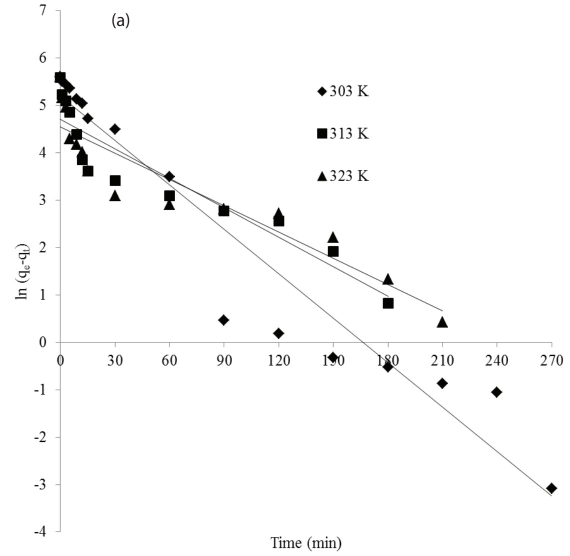

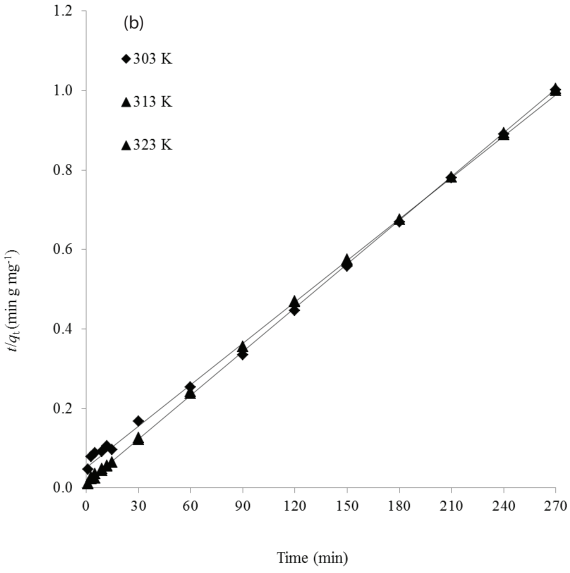

Fig. 9. Kinetic profiles for the adsorption of MB onto PAC at variable temperature: (a) pseudo-first-order and (b) pseudo-second-order models.

Table 4
Comparison of the pseudo-first-order (PFO) and pseudo-second-order (PSO) models for the adsorption of MB on PAC at variable temperatures

	Temperature (K)		
	303	313	323
$q_{e,\text{exp.}}$	269.74	268.65	270.17
PFO			
$q_{e,\text{cal.}}$	181.53	111.50	94.65
k_1 (min^{-1})	0.078	0.021	0.019
R^2	0.940	0.866	0.863
PSO			
$q_{e,\text{cal.}}$	285.71	270.27	270.27
$k_2 \times 10^{-3}$	0.20	0.85	1.01
R^2	0.998	0.999	0.999

Table 5
Thermodynamic parameters values for the adsorption of MB onto PAC

Temperature (K)	Thermodynamics parameters			
	K_d	$\Delta G°$ (kJ/mol)	$\Delta H°$ (kJ/mol)	$\Delta S°$ (J/mol K)
			21.91	109.59
303	86.66	–55.11		
313	122.79	–56.21		
323	148.26	–57.30		

temperature (K). The values of $\Delta H°$ and $\Delta S°$ were calculated from the slope and intercept of van't Hoff plots of lnK_d vs. 1/T, respectively. The thermodynamic parameters are listed in Table 5. The values of $\Delta G°$ of MB adsorption at the temperature of 303, 313 and 323 K were determined as –55.11, –56.21 and –57.30 kJ/mol, respectively. As stated by Jaycock and Parfitt [52], the value for $\Delta G°$, energy for physisorption ranges from –20 to 0 kJ/mol, the physisorption together with chemisorption falls at the range of –20 to –80 kJ/mol and chemisorption is in the range of –80 to –400 kJ/mol. Thus, the MB adsorption by PAC shows both physisorption and chemisorption properties. The negative values of $\Delta G°$ indicate spontaneous and favorable MB adsorption onto the surface of PAC. According to Noll et al. [53] the enthalpy for physisorption is normally below 0 kJ/mol, while for the chemisorption is in the range of –80 to –420 kJ/mol. The calculated $\Delta H°$ value was +21.91 kJ/mol indicating that the adsorption process is endothermic in nature. The positive value of $\Delta S°$ (109.59 J/(mol K)) shows that the affinity of PAC to MB and its randomness at the solid/solution interface increases during the adsorption process [54].

4. Conclusion

This study investigates the feasibility of coconut leaves as a new and low cost precursor for the preparation of activated carbon using H_3PO_4 as an activator via thermal method. PAC has high BET surface area and total pore volume of 981.79 m^2/g and 1.371 cm^3/g, respectively. The adsorption experiments indicated that the adsorption equilibrium data were better simulated by the Langmuir model with maximum adsorption capacity of 357.14 mg/g at 303 K and 370.37 mg/g at temperature of 313 and 323 K, respectively. On the other hand, the PSO model provided the best kinetic model for the system. The thermodynamic parameters indicate that the adsorption process is endothermic and driven by entropy to yield a spontaneous adsorption process. The results indicated that PAC is an efficient adsorbent for MB adsorption.

Acknowledgments

The authors would like to thank the Ministry of Education, Malaysia for funding this research work under the Research Acculturation Grant Scheme (600-RMI/RAGS 5/3(18/2014)). The authors also thank the Research Management Institute (RMI) and the Universiti Teknologi MARA for supporting the research work.

References

[1] A.H. Jawad, R.A. Rashid, M.A.M. Ishak, L.D. Wilson, Adsorption of methylene blue onto activated carbon developed from biomass waste by H_2SO_4 activation: kinetic, equilibrium and thermodynamic studies, Desal. Wat. Treat., 57 (2016) 25194–25206.

[2] R.A. Rashid, A.H. Jawad, M.A.M. Ishak, N.N. Kasim, KOH-activated carbon developed from biomass waste: adsorption equilibrium, kinetic and thermodynamic studies for Methylene blue uptake, Desal. Wat. Treat., 57 (2016) 27226–27236.

[3] S. Ismadji, Y. Sudaryanto, S.B. Hartono, L.E.K. Setiawan, A. Ayucitra, Activated carbon from char obtained from vacuum pyrolysis of teak sawdust: pore structure development and characterization, Bioresour. Technol., 96 (2005) 1364–1369.

[4] C.P. Huang, Carbon Adsorption Handbook, 2nd ed., Ann Arbor Science Publishers Inc., Michigan, 1980.

[5] K. Li, Z. Zheng, Y. Li, Characterization and lead adsorption properties of activated carbons prepared from cotton stalk by one-step H_3PO_4 activation, J. Hazard. Mater., 181 (2010) 440–447.

[6] S. Yorgun, N. Vural, H. Demiral, Preparation of high-surface area activated carbons from Paulownia wood by $ZnCl_2$ activation, Microporous Mesoporous Mater., 122 (2009) 189–194.

[7] A.H. Jawad, N.F.H. Mamat, M.F. Abdullah, K. Ismail, Adsorption of methylene blue onto acid-treated mango peels: kinetic, equilibrium and thermodynamic study, Desal. Wat. Treat., 59 (2017) 210–219.

[8] I. Okman, S. Karagöz, T. Tay, M. Erdem, Activated carbons from grape seeds by chemical activation with potassium carbonate and potassium hydroxide, Appl. Surf. Sci., 293 (2014) 138–142.

[9] M. Hejazifar, S. Azizian, H. Sarikhani, Q. Li, D. Zhao, Microwave assisted preparation of efficient activated carbon from grapevine rhytidome for the removal of methyl violet from aqueous solution, J. Anal. Appl. Pyrolysis, 92 (2011) 258–266.

[10] T. Ramesh, N. Rajalakshmi, K.S. Dhathathreyan, Activated carbons derived from tamarind seeds for hydrogen storage, J. Energy Storage, 4 (2015) 89–95.

[11] E.N. El Qada, S.J. Allen, G.M. Walker, Influence of preparation conditions on the characteristics of activated carbons produced in laboratory and pilot scale systems, Chem. Eng. J., 142 (2008) 1–13.

[12] A. Sivapragasam, Paper Presented at the Second International Plantation Industry Conference and Exhibition (IPICEX2008), Shah Alam, Malaysia, 2008.

[13] T. Tahir, F. Hamid, Vermicomposting of two types of coconut wastes employing *Eudrilus eugeniae*: a comparative study, Int. J. Recycl. Org. Waste Agric., 1 (2012) 1–6.

[14] K.Y. Foo, B.H. Hameed, Textural porosity, surface chemistry and adsorptive properties of durian shell derived activated carbon prepared by microwave assisted NaOH activation, Chem. Eng. J., 187 (2012) 53–62.

[15] A.U. Isah, G. Abdulraheem, S. Bala, S. Muhammad, M. Abdullahi, Kinetics, equilibrium and thermodynamics studies of C.I. Reactive Blue 19 dye adsorption on coconut shell based activated carbon, Int. Biodeterior. Biodegrad., 102 (2015) 265–273.

[16] V.O. Njoku, M.A. Islam, M. Asif, B.H. Hameed, Preparation of mesoporous activated carbon from coconut frond for the adsorption of carbofuran insecticide, J. Anal. Appl. Pyrolysis, 110 (2014) 172–180.

[17] A. Kamari, S.N.M. Yusoff, F. Abdullah, W.P. Putra, Biosorptive removal of Cu(II), Ni(II) and Pb(II) ions from aqueous solutions using coconut dregs residue: adsorption and characterisation studies, J. Environ. Chem. Eng., 2 (2014) 1912–1919.

[18] A.H. Jawad, R.A. Rashid, R.M.A. Mahmuod, M.A.M. Ishak, N.N. Kasim, K. Ismail, Adsorption of methylene blue onto coconut (*Cocos nucifera*) leaf: optimization, isotherm and kinetic studies, Desal. Wat. Treat., 57 (2016) 8839–8853.

[19] A.H. Jawad, A.F.M. Alkarkhi, N.S.A. Mubarak, Photocatalytic decolorization of methylene blue by an immobilized TiO_2 film under visible light irradiation: optimization using response surface methodology (RSM), Desal. Wat. Treat., 56 (2015) 161–172.

[20] A.H. Jawad, N.S.A. Mubarak, M.A.M. Ishak, K. Ismail, W.I. Nawawi, Kinetics of photocatalytic decolourization of cationic dye using porous TiO_2 film, J. Taibah Univ. Sci., 10 (2016) 352–362.

[21] N.S.A. Mubarak, A.H. Jawad, W.I. Nawawi, Equilibrium, kinetic and thermodynamic studies of Reactive Red 120 dye adsorption by chitosan beads from aqueous solution, Energy Ecol. Environ., 2 (2017) 85–93.

[22] A.H. Jawad, M.A. Islam, B.H. Hameed, Cross-linked chitosan thin film coated onto glass plate as an effective adsorbent for adsorption of reactive orange 16, Int. J. Biol. Macromol., 95 (2017) 743–749.

[23] M.J. Ahmed, S.K. Dhedan, Equilibrium isotherms and kinetics modeling of methylene blue adsorption on agricultural wastes-based activated carbons, Fluid Phase Equilib., 317 (2012) 9–14.

[24] M. Makeswari, T. Santhi, Optimization of preparation of activated carbon from *Ricinus communis* leaves by microwave-assisted zinc chloride chemical activation: competitive adsorption of Ni^{2+} ions from aqueous solution, J. Chem., 2013 (2013) 314790. Available at: http://dx.doi.org/10.1155/2013/314790.

[25] V.O. Njoku, K.Y. Foo, B.H. Hameed, Microwave-assisted preparation of pumpkin seed hull activated carbon and its application for the adsorptive removal of 2,4-dichlorophenoxyacetic acid, Chem. Eng. J., 215–216 (2013) 383–388.

[26] M.A. Islam, M.J. Ahmed, W.A. Khanday, M. Asif, B.H. Hameed, Mesoporous activated carbon prepared from NaOH activation of rattan (*Lacosperma secundiflorum*) hydrochar for methylene blue removal, Ecotoxicol. Environ. Saf., 138 (2017) 279–285.

[27] K.V. Kumar, C.V. Calahorro, J.M. Juarez, M.M. Sabio, J.S. Albero, F.R. Reinoso, Hybrid isotherms for adsorption and capillary condensation of N_2 at 77 K on porous and non-porous materials, Chem. Eng. J., 162 (2010) 424–429.

[28] K.S.W. Sing, D.H. Everett, R.A.W. Haul, L. Moscou, R.A. Pierotti, J. Rouquérol, T. Siemieniewska, Reporting physisorption data for gas/solid systems with special reference to the determination of surface area and porosity, Pure Appl. Chem., 57 (1985) 603–619.

[29] R.L. Burwell, Manual of Symbols and Terminology for Physicochemical Quantities and Units, Appendix II, Definitions, Terminology and Symbols in Colloid and Surface Chemistry, International Union of Pure and Applied Chemistry (IUPAC) Vol. 31, 1972, pp. 578–638.

[30] S. Uçar, M. Erdem, T. Tay, S. Karago, Preparation and characterization of activated carbon produced from pomegranate seeds by $ZnCl_2$ activation, Appl. Surf. Sci., 255 (2009) 8890–8896.

[31] M.D. Pavlović, A.V. Buntić, K.R. Mihajlovski, S.S. Šiler-Marinković, D.G. Antonović, Ž. Radovanović, S.I. Dimitrijević-Branković, Rapid cationic dye adsorption on polyphenol-extracted coffee grounds—a response surface methodology approach, J. Taiwan Inst. Chem. Eng., 45 (2014) 1691–1699.

[32] M. Benadjemia, L. Millière, L. Reinert, N. Benderdouche, L. Duclaux, Preparation, characterization and Methylene Blue adsorption of phosphoric acid activated carbons from globe artichoke leaves, Fuel Process. Technol., 92 (2011) 1203–1212.

[33] A. Reffas, V. Bernardet, B. David, L. Reinert, M.B. Lehocine, M. Dubois, N. Batisse, L. Duclaux, Carbons prepared from coffee grounds by H_3PO_4 activation: characterization and adsorption of methylene blue and Nylosan Red N-2RBL, J. Hazard. Mater., 175 (2010) 779–788.

[34] K.C. Bedin, A.C. Martins, A.L. Cazetta, O. Pezoti, V.C. Almeida, KOH-activated carbon prepared from sucrose spherical carbon: adsorption equilibrium, kinetic and thermodynamic studies for Methylene Blue removal, Chem. Eng. J., 286 (2015) 476–484.

[35] H. Lata, V.K. Garg, R.K. Gupta, Removal of a basic dye from aqueous solution by adsorption using *Parthenium hysterophorus*: an agricultural waste, Dye Pigm., 74 (2007) 653–658.

[36] V.K. Garg, R. Kumar, R. Gupta, Removal of malachite green dye from aqueous solution by adsorption using agro-industry waste: a case study of *Prosopis cineraria*, Dye Pigm., 62 (2004) 1–10.

[37] M.C. Ncibi, B. Mahjoub, M. Seffen, Kinetic and equilibrium studies of methylene blue biosorption by *Posidonia oceanica* (L.) fibres, J. Hazard. Mater., 139 (2007) 280–285.

[38] Y. Shen, S. Wang, Y. Tzou, Y. Yan, W. Kuan, Removal of hexavalent Cr by coconut coir and derived chars – the effect of surface functionality, Bioresour. Technol. 104 (2012) 165–172.

[39] I. Langmuir, The adsorption of gases on plane surfaces of glass, mica and platinum, J. Am. Chem. Soc., 40 (1918) 1361–1403.

[40] H. Freundlich, Ueber die adsorption in Loesungen (Adsorption in solution), Z. Phys. Chem., 57 (1906) 385–470.

[41] A.M.M. Vargas, A.L. Cazetta, M.H. Kunita, T.L. Silva, V.C. Almeida, Adsorption of methylene blue on activated carbon produced from flamboyant pods (*Delonix regia*): study of adsorption isotherms and kinetic models, Chem. Eng. J., 168 (2011) 722–730.

[42] T. Ibrahim, B.L. Moctar, K. Tomkouani, D. Gbandi, D.K. Victor, N. Phinthè, Kinetics of the adsorption of anionic and cationic dyes in aqueous solution by low-cost activated carbons prepared from shea cake and cotton cake, Am. Chem. Sci. J., 4 (2014) 38–57.

[43] H. Deng, G. Zhang, X. Xu, G. Tao, J. Dai, Optimization of preparation of activated carbon from cotton stalk by microwave assisted phosphoric acid-chemical activation, J. Hazard. Mater., 182 (2010) 217–224.

[44] S. Senthilkumaar, P.R. Varadarajan, K. Porkodi, C.V. Subbhuraam, Adsorption of methylene blue onto jute fiber carbon: kinetics and equilibrium studies, J. Colloid Interface Sci., 284 (2005) 78–82.

[45] Q.S. Liu, T. Zheng, N. Li, P. Wang, G. Abulikemu, Modification of bamboo-based activated carbon using microwave radiation and its effects on the adsorption of methylene blue, Appl. Surf. Sci., 256 (2010) 3309–3315.

[46] G.O. El-Sayed, M.M. Yehia, A.A. Asaad, Assessment of activated carbon prepared from corncob by chemical activation with phosphoric acid, Water Resour. Ind., 7–8 (2014) 66–75.

[47] S. Lagergren, About the theory of so called adsorption of soluble substances, K. Sven. Vetensk.akad. Handl., 24 (1898) 1–39.

[48] Y.S. Ho, G. McKay, Sorption of dye from aqueous solution by peat, Chem. Eng. J., 70 (1998) 115–124.

[49] A. Islam, I.A.W. Tan, A. Benhouria, M. Asif, B.H. Hameed, Mesoporous and adsorptive properties of palm date seed activated carbon prepared via sequential hydrothermal carbonization and sodium hydroxide activation, Chem. Eng. J., 270 (2015) 187–195.

[50] C. Djilani, R. Zaghdoudi, F. Djazi, B. Bouchekima, A. Lallam, A. Modarressi, M. Rogalski, Adsorption of dyes on activated carbon prepared from apricot stones and commercial activated carbon, J. Taiwan Inst. Chem. Eng., 53 (2015) 112–121.

[51] J.J. Gao, Y.B. Qin, T. Zhou, D.D. Cao, P. Xu, D. Hochstetter, Y.F. Wang, Adsorption of methylene blue onto activated carbon produced from tea (*Camellia sinensis* L.) seed shells: kinetics, equilibrium, and thermodynamics studies, J. Zhejiang Univ. Sci. B, 14 (2013) 650–658.

[52] M.J. Jaycock, G.D. Parfitt, Chemistry of Interfaces, Ellis Horwood Ltd., Onichester, 1981.

[53] K.E. Noll, V. Gounaris, W.S. Hou, Adsorption Technology for Air and Water Pollution Control, Lewis Publishers, Chelsea, MI, 1992, pp. 21–22.

[54] I.A.W. Tan, A.L. Ahmad, B.H. Hameed, Adsorption of basic dye on high-surface-area activated carbon prepared from coconut husk: equilibrium, kinetic and thermodynamic studies, J. Hazard. Mater., 154 (2008) 337–346.